An ionic liquid-gated polymer thin film transistor with exceptionally low "on" resistance

Saud A. Algarni, Talal M. Althagafi, Patrick J. Smith, and Martin Grell

An ionic liquid-gated polymer thin film transistor with exceptionally low "on" resistance

Saud A. Algarni,[1,a)] Talal M. Althagafi,[1] Patrick J. Smith,[2] and Martin Grell[1]

[1]*Department of Physics and Astronomy, University of Sheffield, Hicks Building, Hounsfield Rd, Sheffield S3 7RH, United Kingdom*
[2]*Laboratory of Applied Inkjet Printing, Department of Mechanical Engineering, Gladstone Building, Garden Street, University of Sheffield, Sheffield S1 4BA, United Kingdom*

We report the ionic liquid (IL) gating of a solution processed semiconducting polymer, poly(2,5-bis(3-hexadecylthiophen-2-yl)thieno[3,2-b]thiophene) (PBTTT). IL gating relies on the poor solubility of PBTTT, which requires hot chlorinated benzenes for solution processing. PBTTT, thus, resists dissolution even in IL, which otherwise rapidly dissolves semiconducting polymers. The resulting organic thin film transistors (OTFTs) display low threshold, very high carrier mobility (>3 cm^2/Vs), and deliver high currents (in the order of 1 mA) at low operational voltages. Such OTFTs are interesting both practically, for the addressing of current-driven devices (e.g., organic LEDs), and for the study of charge transport in semiconducting polymers at very high carrier density. © 2014 AIP Publishing LLC. [http://dx.doi.org/10.1063/1.4875746]

Much of the attraction of using organic semiconductors (OSCs) comes from their processing options: semiconducting polymers, in particular, can often be processed from solutions. To maximise processing advantages, all device components, not just the semiconductor, should be solution processed. A limiting factor, however, is the generally lower charge carrier mobility in OSCs, compared to conventional semiconductors. This is an issue in applications where organic thin film transistors (OTFTs) have to supply current, e.g., to drive organic light emitting diodes. Maximising the current delivered by solution-processed OTFTs is thus the subject of many studies, including this letter. Equation (1) provides a guideline towards high current OTFTs that work at moderate operational voltages

$$I_{D,sat} = \frac{W}{2L} \mu C_i (V_G - V_T)^2 . \qquad (1)$$

Wherein, the saturated drain current $I_{D,sat}$ is the highest current an OTFT can deliver at a given gate voltage, V$_G$.[1] W/L stands for the width/length of the OTFT channel, μ for the semiconductor's charge carrier mobility, C_i for the gate medium's specific capacitance, and V_T for the OTFT threshold voltage. Clearly, high mobility semiconductors, combined with high capacitance gate media and low threshold maximise drain current for a given gate voltage. However, parameters μ, C_i, and V_T are convoluted, e.g., high C_i leads to reduced V_T, but may rely on polar gate media that reduce μ.[2] Also, every gate medium has a limited stability to applied voltages (dielectric breakdown for insulating gate media, electrochemical window for electrolytes). Hence, V_G is limited to a practical maximum, V_G (max). As the geometry factor W/L is somewhat arbitrary, we define two figures-of-merit independent of W/L to quantify the ability of an OTFT

to deliver current, namely the maximum sheet current I_W, and the lowest sheet resistance R_W, according to Eq. (2)

$$I_W = \frac{L}{W} I_{D,sat}(V_G = V_G(max)), \qquad (2a)$$

$$R_W = \frac{V_G(max)}{I_W}. \qquad (2b)$$

In recent years, OTFTs using electrolytes rather than insulators as gate media have been demonstrated, including solid electrolytes,[3,4] water,[5,6] and ionic liquids (ILs).[7–9] Under applied gate voltage, an extremely thin electric double layer (EDL) forms at the electrolyte/semiconductor interface, with high specific capacitance (>1000 nF/cm^2), low V_T, and consequently high I_W/low R_W. Ionic liquids (ILs) lead to particularly high C_i, and display key practical advantages over aqueous electrolytes: ILs are not volatile,[10] and IL/polymer formulations can be inkjet printed and subsequently gel into a quasi- solid film.[11] However, ILs are excellent solvents,[10] and thus not generally suited for use with solution processed OSCs- previous reports of IL- gated OTFTs used vacuum evaporated OSCs only.[7–9]

Here, we report on an OTFT that uses a solution-processed polymer OSC in conjunction with an IL gate medium. We used the polymer OSC poly(2,5-bis(3-hexadecylthiophen-2-yl)thieno[3,2-b]thiophene) (PBTTT), Fig. 1(a), which is known for its exceptionally high carrier mobility.[4,12] Also, due to its particularly rigid conjugated backbone, PBTTT only dissolves in hot chlorinated benzenes.[12] We here show that PBTTT's poor solubility extends to an IL, 1-ethyl-3-methylimidazolium-bis(trifluoromethyl-sulfonyl)imide ("EMITSFI") Fig. 1(b), which had previously been used as gate medium for evaporated OSCs.[7,9] Resulting OTFTs display good figures- of- merit I_W and R_W.

For OTFT fabrication, we used prefabricated gold source/drain (S/D) contact substrates of W = 2 mm/L = 10 μm (W/L = 200) described previously,[6] and inkjet printed silver

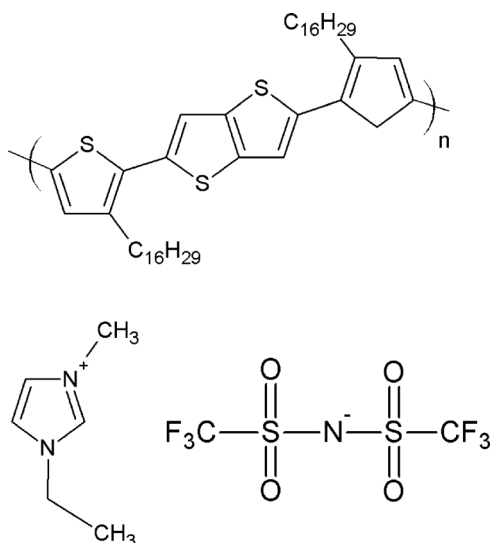a)Author to whom correspondence should be addressed. Electronic mail: Php11saa@sheffield.ac.uk

FIG. 1. Chemical structures of semiconducting polymer PBTTT, and ionic liquid EMITFSI.

(Ag) contacts of $W = 3\,mm\,/\,L = 40\,\mu m$ ($W/L = 75$) printed from a 20 wt. % suspension of silver nanoparticles (size ranged 20–50 nm) in ethanol and ethylene glycol (from Sun Chemical, Slough, GB), similar to a procedure reported

previously.[13,14] Ink viscosity and surface tension were 12 mPa s and 27–31 mN/m at room temperature, respectively. We used a JetLab 4xl printing system (Microfab, Inc., Plano, TX), equipped with a 60 μm diameter drop-on-demand piezoelectric printhead (MJ-AT-01-60, Microfab, Inc.). Printing frequency was set at 100 Hz, voltage to 60 V, and a pulse width to 10 μs. Printing was performed at room temperature onto glass substrates previously cleaned with acetone and isopropanol. Printed contact substrates were allowed to dry at room temperature for 10 min before being placed on a hotplate at 200 °C for 60 min to remove the carrier solvent and organic components and sinter the silver nanoparticles. (An image of the printed S/D substrates is shown as an inset in Fig. 3(b)). The resistance between the pad for external contacting, and the "source" contact to the OTFT channel, was measured as $\sim 40\,\Omega$. 7 mg/ml PBTTT sourced from Ossila Ltd was dissolved by stirring into hot 1,2 dichlorobenzene (DCB) (110 °C) for 45 min, and spun onto contact substrates from hot (100 °C) DCB for 40s at 5000 rpm. After casting, films were dried under dynamic vacuum at 110 °C for 1 h. For electrolyte gating, we applied droplets (5-8 μl) of EMITSFI IL (sourced from Aldrich), or DI water, from a microlitre syringe over the channel area, and inserted an Au gate needle (American Probe and Technologies) bent into L- shape. For

FIG. 2. (a) Output characteristics for IL- gated PBTTT OTFT with Au source/drain contacts. (b) Saturated transfer characteristics (red short dash), parameteric in time, for same device. Also shown is the saturated transfer characteristic for same device when gated with water (green long dash). The drive voltage, applied to the source, is shown in solid blue.[16]
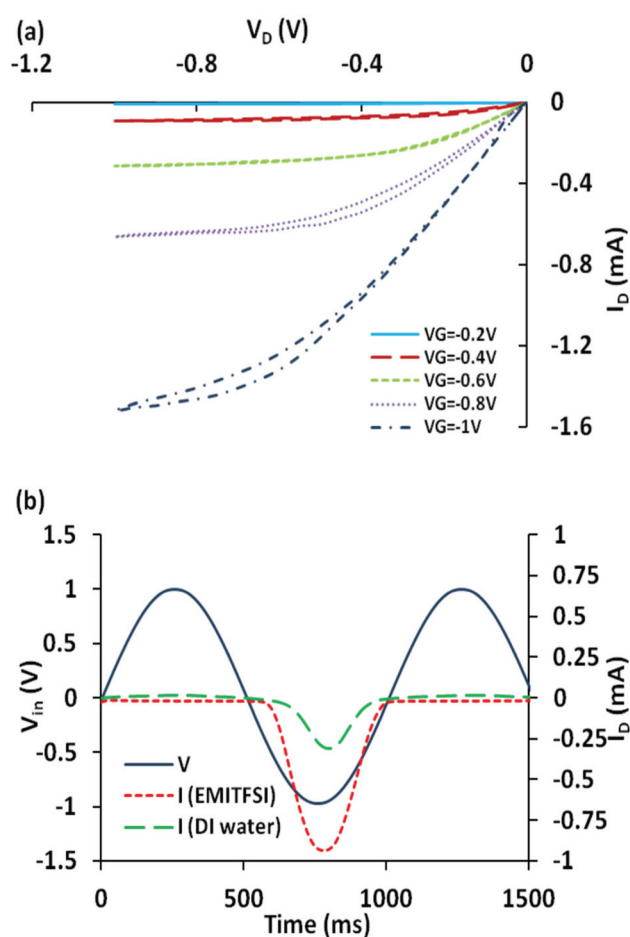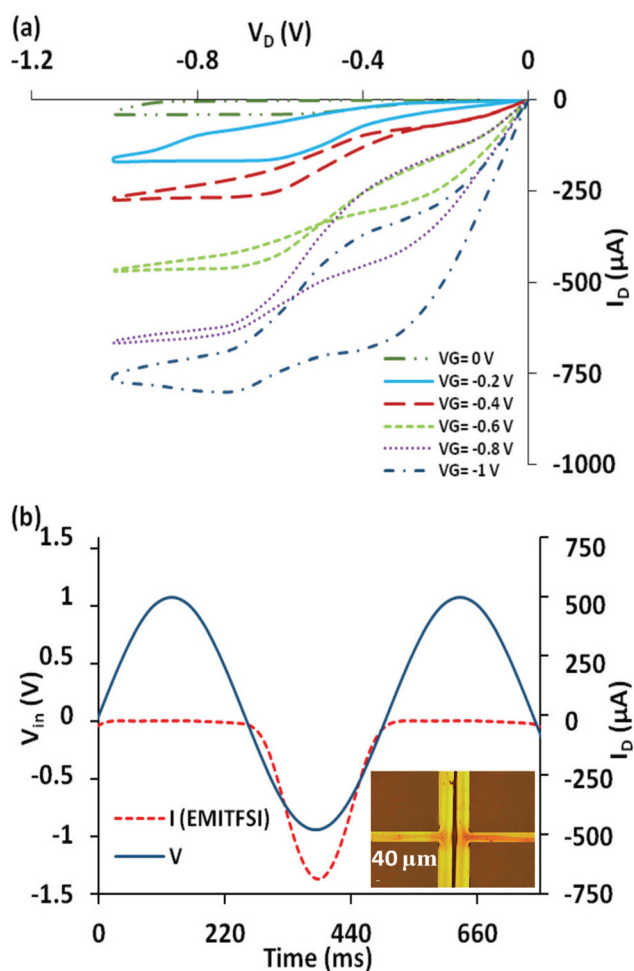

FIG. 3. (a) Output characteristics for IL- gated PBTTT OTFT with printed Ag source/drain contacts. (b) Saturated transfer characteristics (red short dash), parametric in time, for same device. Drive voltage in solid blue. Inset: Optical micrograph of printed/fused Ag contacts; $L = 40\,\mu m$.

TABLE I. Figures- of- merit I_W and R_W (Eq. (2)) from recent publications, in comparison to data from this work. We include a range of semiconductors (solution processed and evaporated), and gate media (dielectrics, solid electrolytes, liquid electrolytes). We calculated I_W and R_W from characteristics shown in the respective publications.

References	Semiconductor	Deposition	h⁺/e⁻	Gate medium	I_W [μA/□]	R_W [MΩ/□]
Hasegawa et al.[21]	C_8-BTBT	Ink jet (2 shot)	h⁺	Dielectric	69	0.87
Klauk et al.[22]	DNTT	Evaporation	h⁺	Dielectric	0.54	5.56
Bao et al.[23]	Pentacene	Evaporation	h⁺	Dielectric	0.3	6.7
Horowitz et al.[5]	P3HT	Spin casting	h⁺	Water	0.0054	111
Grell et al.[6]	ACN- conditioned BBL nanobelts	Drop casting	e⁻	Water	0.35	2.28
Berggren et al.[3]	P3HT	Spin casting	h⁺	Solid electrolyte	0.0175	57
Frisbie et al.[3] Takeya et al.[7]	Rubrene	Evaporation	h⁺	Ionic liquid	0.66	0.3
Takeya et al.[9]	C_{60}	Evaporation	e⁻	Ionic Liquid	0.027	37
Heeney et al.[12]	PBTTT	Spin casting	h⁺	Dielectric	25	2.4
Torsi et al.[4]	PBTTT	Spin casting	h⁺	Solid electrolyte	0.459	2.18
This work	PBTTT (Au contacts)	Spin casting	h⁺	Ionic Liquid	7.6	0.132
This work	PBTTT (inkjet Ag contacts)	Spin casting	h⁺	Ionic Liquid	9.7	0.102
This work	PBTTT (Au contacts)	Spin casting	h⁺	Water	1.6	0.64

electrical characterisation, we used either a setup consisting of two Keithley 4200 source/measure units[15] (for output characteristics), or a bespoke current/voltage (I/V) converter setup described previously[6,16–18] for saturated transfer characteristics. All measurements were carried out under ambient atmosphere.

Figs. 2(a) and 2(b) shows output characteristics, and saturated transfer characteristics, of an IL- gated PBTTT OTFT with Au contacts. Note that the transfer characteristic is shown parametric in time, rather than explicitly. The acquisition and evaluation of parametric transfer characteristics, and the reasons for doing so, were discussed in detail previously[6,16–18] The PBTTT OTFT output characteristics display near- ideal shape, with little hysteresis and linear $I_D(V_D)$ behaviour for low V_D, which indicates good hole injection at the Au/PBTTT source contacts ("ohmic contacts"). At large negative V_D and V_G, I_D saturates; at $V_G = V_D = -1V$, we observe a drain current of $|I_D| = 1.52$ mA, which according to Eq. (2) gives $I_W = 7.6 \, \mu A/\square$ and $R_W = 131.6 \, k\Omega/\square$. This is an exceptionally low OTFT sheet resistance, in comparison to other recent reports, cited in Table I, of high performance OTFTs. Like Regioregular poly(3-hexylthiophene-2,5-diyl) (P3HT),[5] PBTTT can also be gated with deionised water, an example is included in Fig. 2(b). Resulting drain currents are lower than for IL gating, but significantly larger than for water- gated P3HT.[5]

In a control experiment with IL on a blank contact substrate without OSC, we found maximum currents of only 0.45 μA. We can therefore safely exclude that parasitic currents in the IL account for the observed characteristics.

Charge carrier mobility in the saturated regime μ_{sat}, and threshold voltage V_T, can be evaluated from the saturated transfer characteristics in Fig. 2(b) by eliminating time, and plotting in the form $I_D^{1/2}$ vs V_G.[16] A straight line fit gives threshold from the intercept with the V_G- axis, and μ_{sat} from the slope, cf. Eq. (1). We find $V_T = -0.36$ V for IL gating. To evaluate μ_{sat}, we assume specific capacitance of $C_i \sim 7000$ nF/cm², reported by Ono et al.[7] for the IL EMITFSI at low frequency (1 Hz). We find $\mu_{sat} = 3.24$ cm²/Vs, a remarkable

carrier mobility for a polymer OSC. However, PBTTT is already known for its exceptional mobility, e.g., Hamadani et al. report a mobility of ~ 1 cm²/Vs for dielectric- gated PBTTT OTFTs.[12] In addition, gating with a high capacitance IL leads to very high charge carrier density in the accumulation layer, and it is known that mobility increases at high carrier density.[19]

When we measure saturated transfers on IL- gated PBTTT with drive voltages in excess of 1.2 V, we soon find a decline in on/off ratio (on/off ~ 2200 under 1 V drive), and rapid decay in overall device performance. We believe this decline is related to the electrolysis of water: The highly hygroscopic IL will rapidly absorb water from atmospheric humidity, and while the "electrochemical window" of the EMITSFI IL used here is 4.3 V,[10] it is only 1.23 V for water. We therefore limited ourselves to a maximum of 1 V in subsequent experiments. Limiting gate voltage to 1 V is not a serious drawback though: Xie and Frisbie have recently reported that mobility declines again in IL- gated devices at gate voltages >1 V,[8] probably due a binding between holes in the OSC and anions in the IL.

Realistic "printed electronics" requires solution processing of all OTFT components, including the S/D contacts. We have therefore also prepared IL-gated PBTTT OTFTs with printed Ag contacts. Characteristics are shown in Fig. 3.

Output characteristics Fig. 3(a) display significant hysteresis, and for low gate voltages, $I_D(V_D)$ at low drain voltage is not linear, but I_D remains sublinear initially and curves upwards only at higher V_D. Such sub- linear shape is the signature of a significant hole injection barrier at the printed Ag/PBTTT contact, due to the lower work function of Ag compared to Au. The exceptionally high conductivity of the IL- gated channel exacerbates the poor contacts, leading to highly non-ideal output characteristics. However, at higher gate voltages, the injection problem at the contact is resolved, probably because the high gate voltage strongly assists tunnelling injection. Therefore, IL-gated PBTTT with printed Ag contacts deliver high drain currents at $V_G = V_D = -1V$. In fact, sheet current is higher ($I_W = 9.7 \, \mu A/\square$ vs.

$I_W = 7.6\,\mu\text{A/}\square$) and sheet resistance lower ($R_W = 102\,\text{k}\Omega/\square$ vs. $R_W = 131.6\,\text{k}\Omega/\square$) than for OTFTs with Au S/D contacts, despite the injection barrier at the Ag contact. It is known, however, that apparent carrier mobility (and hence, sheet current), increases for longer channel length, L, because the relative contribution of contact resistance is diluted by longer channels, even when contacts are ohmic.[20] The dependence of apparent mobility on L casts some doubt on the sheet current/sheet resistance metric in general, but it is nevertheless widely used for characterising conductive surfaces, e.g., synthetic metal films.

To summarise, we report the IL gating of a solution processed semiconducting polymer, PBTTT. Performance of resulting OTFT devices is shown in Table I, in the form I_W and R_W, in comparison to a few high- performance OTFTs from the recent literature.

Our figures-of-merit for entirely solution-processed OTFTs compare favourably within Table I, which is the result of the concurrent high capacitance, high carrier mobility, and low threshold, of the PBTTT/EMITSFI EDL transistor. Also, IL gating of PBTTT allows exploring the intriguing physics of OSCs at extremely high charge carrier concentrations[8] on the example of a semiconducting polymer. As a concluding remark, we note that currently, the operational lifetime of the devices introduced here is still limited to not much longer than 1 h, probably due to an eventual slow dissolution of PBTTT in IL. Limited durability warrants further improvement, e.g., by the use of a gelled IL,[11] or synthesis of a PBTTT derivative that can be cross-linked after deposition.

[1]G. Horowitz, in *Semiconducting Polymers*, edited by G. Hadziioannou and P. F. Van Hutten (Wiley-VCH Verlag GmbH & Co. KGaA, Weinheim, 2000), p. 463.

[2]J. Veres, S. D. Ogier, S. W. Leeming, D. C. Cupertino, and S. M. Khaffaf, Adv. Funct. Mater. **13**(3), 199 (2003).

[3]E. Said, X. Crispin, L. Herlogsson, S. Elhag, N. D. Robinson, and M. Berggren, Appl. Phys. Lett. **89**(14), 143507 (2006).

[4]L. M. Dumitru, K. Manoli, M. Magliulo, L. Sabbatini, G. Palazzo, and L. Torsi, ACS Appl. Mater. Interfaces **5**(21), 10819 (2013).

[5]L. Kergoat, L. Herlogsson, D. Braga, B. Piro, M. Pham, X. Crispin, M. Berggren, and G. Horowitz, Adv. Mater. **22**(23), 2565 (2010).

[6]A. Al Naim, A. Hobson, R. T. Grant, A. Dragoneas, M. Hampton, C. Dunscombe, T. Richardson, J. E. Macdonald, and M. Grell, Org. Electron. **14**(4), 1057 (2013).

[7]S. Ono, S. Seki, R. Hirahara, Y. Tominari, and J. Takeya, Appl. Phys. Lett. **92**(10), 103313 (2008).

[8]W. Xie and C. D. Frisbie, J. Phys. Chem. C **115**(29), 14360 (2011).

[9]T. Uemura, M. Yamagishi, S. Ono, and J. Takeya, Appl. Phys. Lett. **95**(10), 103301 (2009).

[10]R. Hagiwara and Y. Ito, J. Fluorine Chem. **105**(2), 221 (2000).

[11]U. Löffelmann, N. Wang, D. Mager, P. J. Smith, and J. G. Korvink, J. Polym. Sci., Part B: Polym. Phys. **50**(1), 38 (2012).

[12]B. H. Hamadani, D. J. Gundlach, I. McCulloch, and M. Heeney, Appl. Phys. Lett. **91**(24), 243512 (2007).

[13]H. Meier, U. Löffelmann, D. Mager, P. J. Smith, and J. G. Korvink, Phys. Status Solidi A **206**(7), 1626 (2009).

[14]D.-Y. Shin and P. J. Smith, J. Appl. Phys. **103**(11), 114905 (2008).

[15]L. A. Majewski, R. Schroeder, M. Voigt, and M. Grell, J. Phys. D: Appl. Phys. **37**(24), 3367 (2004).

[16]L. Hague, D. Puzzovio, A. Dragoneas, and M. Grell, Sci. Adv. Mater. **3**, 907 (2011).

[17]L. Hague, D. Puzzovio, T. H. Richardson, and M. Grell, Sens. Lett. **9**, 1692 (2011).

[18]A. F. Al Naim and M. Grell, J. Appl. Phys. **112**(11), 114502 (2012).

[19]W. F. Pasveer, J. Cottaar, C. Tanase, R. Coehoorn, P. A. Bobbert, P. W. M. Blom, D. M. de Leeuw, and M. A. J. Michels, Phys. Rev. Lett. **94**(20), 206601 (2005).

[20]E. C. P. Smits, S. G. J. Mathijssen, P. A. Van Hal, S. Setayesh, T. C. T. Geuns, K. A. H. A. Mutsaers, E. Cantatore, H. J. Wondergem, O. Werzer, and R. Resel, Nature **455**(7215), 956 (2008).

[21]H. Minemawari, T. Yamada, H. Matsui, J. Tsutsumi, S. Haas, R. Chiba, R. Kumai, and T. Hasegawa, Nature **475**(7356), 364 (2011).

[22]U. Zschieschang, F. Ante, T. Yamamoto, K. Takimiya, H. Kuwabara, M. Ikeda, T. Sekitani, T. Someya, K. Kern, and H. Klauk, Adv. Mater. **22**(9), 982 (2010).

[23]M. E. Roberts, N. Queraltó, S. C. B. Mannsfeld, B. N. Reinecke, W. Knoll, and Z. Bao, Chem. Mater. **21**(11), 2292 (2009).